Journal of Alloys and Compounds 783 (2019) 246–255

Contents lists available at ScienceDirect

Journal of Alloys and Compounds

journal homepage: http://www.elsevier.com/locate/jalcom

Effect of CCBP doping on the multifunctional Al-0.5 Mg-15CCBP superalloy using liquid metallurgy process for advanced application

O.S.I. Fayomi [a, c, *], O.O. Joseph [a], I.G. Akande [b], C.K. Ohiri [a], K.O. Enechi [a], N.E. Udoye [a]

[a] Department of Mechanical Engineering, Covenant University, P.M.B, 1023, Ota, Nigeria
[b] Department of Mechanical Engineering, University of Ibadan, Ibadan, Oyo state, Nigeria
[c] Department of Chemical, Metallurgical and Materials Engineering, Tshwane University of Technology, P.M.B, X680, Pretoria, South Africa

ARTICLE INFO

Article history:
Received 5 December 2018
Received in revised form
24 December 2018
Accepted 26 December 2018
Available online 27 December 2018

Keywords:
Aluminium
Composite
Electrical properties
Mechanical properties
Corrosion

ABSTRACT

One of the greatest challenges of metallic alloys in numerous applications is due to their structural and habitual failure in service. In an attempt to subdue this failure, Aluminium metal matrix composite was developed with the inclusion of carbonized chicken bone powder (CCBP) as the reinforcing particulate. The addition of the nano-sized CCBP was carried out at different percentage weight on an Al6063 alloy. The production of Aluminium metal matrix composite (A6063-CCBP) was achieved using stir casting comprising 0, 5, 10, and 15 wt per cent of CCBP. The electrochemical and weight loss test conducted in 0.5 M of hydrochloric acid on the composite reveal an improved corrosion resistance. Conventional mechanical tests; hardness and tensile test carried out on the composite using Vickers hardness technique and Universal tensile machine respectively showed that the composite now exhibits better mechanical properties. The comparison of the electrical properties from the electrical test carried out pointed to the fact that incorporation of CCBP into Al6063 provided some level of insulation. Also, the morphological change via SEM (Scanning Electron Microscope) micrograph unveiled that the inclusion of CCBP in the A6063 metal matrix reduced cleavages, showing uniform dispersion of the reinforcement along the grain boundaries and more so, minimised brittle fracture.

1. Introduction

The growths of automotive, aerospace and maritime industries have commanded the search for composite materials with good mechanical and chemical properties such as toughness, high hardness and improved corrosion resistance [1–3]. Researches on metal matrix composites in recent years have shown that they exhibit beneficial industrial applications due to their superior strength-to-weight ratio and high resistance to temperature. The development of low-cost materials, especially metal matrix composite with enhanced properties has been the focus of many researchers [4–7]. Regularly, in electrochemically destructive medium like acid and salt, alloys of Aluminium have been used as matrix materials, incorporated with economical reinforcement particles to generate long-lasting aluminium particulate composites [8,9].

Various types of Metal Matrix Composites are fabricated with excellent qualities and continuous configurations and dimensions [10]. Aluminium metal matrix composites (AMMCs) are of immense importance because of their high-temperature capacity as well as thermal stress resistance [11]. Extensive research in the field of AMMCs established beyond suspicion the edges Al-based metal matrix composites (AMMCs) has over the base alloy in the laboratory scale. Today, there is a constant demand for AMMCs for various Engineering components [12]. Carbonized chicken bone powder (CCBP) is known to contain calcium. The calcium content of the bone prevents ignition during casting [13,14]. This is as a result of the retardation in the oxidation rate throughout the melting process by developing tiny and compact calcium oxide layer on the exterior of the melted alloy [15]. The calcium additive further refines the microstructure of the casting as a result of its grain refinement ability [16]. The phosphorus and large carbon content of the ash improves the coalescence of the early stage of the molten metal and hardness of the final composite respectively [17]. The parent aluminium enhance the castability of the entire composite by decreasing the melting point, with the benefit that the overall

* Corresponding author. Department of Mechanical Engineering, Covenant University, P.M.B, 1023, Ota, Nigeria.
E-mail addresses: ojo.fayomi@covenantuniversity.edu.ng, Ojosundayfayomi3@gmail.com, fayomio@tut.ac.za (O.S.I. Fayomi).

https://doi.org/10.1016/j.jallcom.2018.12.312
0925-8388/

alloy strength is not compromised [18]. Magnesium content of the alloy enhances wettability.

Usually, these composites consist of a metal matrix, which is dissolved while casting, and reinforcement which is added to the molten matrix material and stirred mechanical [19]. Amidst the fabrication methods of metal matrix composite, stir casting is regularly preferred. The stir casting liquid transformation method involves the preparation of molten slurry of metals with solid-phase additives of diverse compositions, conveyed and permitted to harden in a die cavity [20]. Its benefits rest on its simplicity, versatility and applicability to a large volume of production. It is also attractive because of the reduced final cost of the product. In the stir casting method, there are many circumstances that require significant consideration, including the challenge of performing a uniform dispersion of the reinforcing particles [21]. Several varieties and volumes of reinforcements were employed in the matrix of Aluminium like SiC, TiC, Al_2O_3, B_4C, TiB_2, TiN, using stir casting method. Amidst these, TiC is a relatively new reinforcement in metal matrix composites and has good properties such as wettability, thermal stability and distribution in Aluminium metal matrix [22–25].

More so, prevailing research has shown that biodegradable agricultural wastes like Carbonized maize stalk particulates and rice husk ash have been utilised to strengthen aluminium alloy [26]. Contrastingly, an attempt to reinforce Aluminium alloy with orange bark ash particulates showed slight reduction in the mechanical properties due to defective adhesion of the reinforcement [27]. This present research employed the use of stir casting technique as a means of reinforcing Aluminium alloys matrix with carbonized chicken bone powder (CCBP). The mass concentration of the carbonized powder was varied and the effect of the reinforced particles was studied using linear potentiodynamic polarization experiment, SEM and Vickers hardness tester.

2. Materials and experimental procedure

2.1. Raw materials

For the fabrication of Al6063-CCBP particulate composite, Al6063 alloy with the chemical composition shown in Table 1 was used as the matrix. The chicken bone waste was carbonized in a closed crucible at a temperature of 400 °C before grinding and screened to an average size of 45 nm as shown in Fig. 2.

2.2. Formation of A6063-CCBP composite slurry by stir casting process

The stir casting set up is presented in Fig. 1. A homogeneous dispersion of CCBP in the Al6063/CCBP composite slurry was carried out by melting Al6603 ingots in the melting chamber and adding the nano sized CCBP in the liquid produced by a mechanical agitator, stirring at a regular speed in the molten Al6063 aluminium alloy [28]. The melted slurry of Al6063 alloy with CCBP was conveyed and left to become solid in the experimental die set. The dispersion of the CCBP in the melted Al6063 matrix is a function of the liquefying temperature, intensity and position of the mechanical stirrer [29].

Table 1
Chemical composition of Al 6063 alloy (wt. %).

Element	S	F	Cu	Mn	Mg	Cr	Ti	Ca	Zr	V	Al
%w	0.157	0.282	0.0025	0.024	0.51	0.023	0.006	0.0011	0.002	0.0035	98.9889

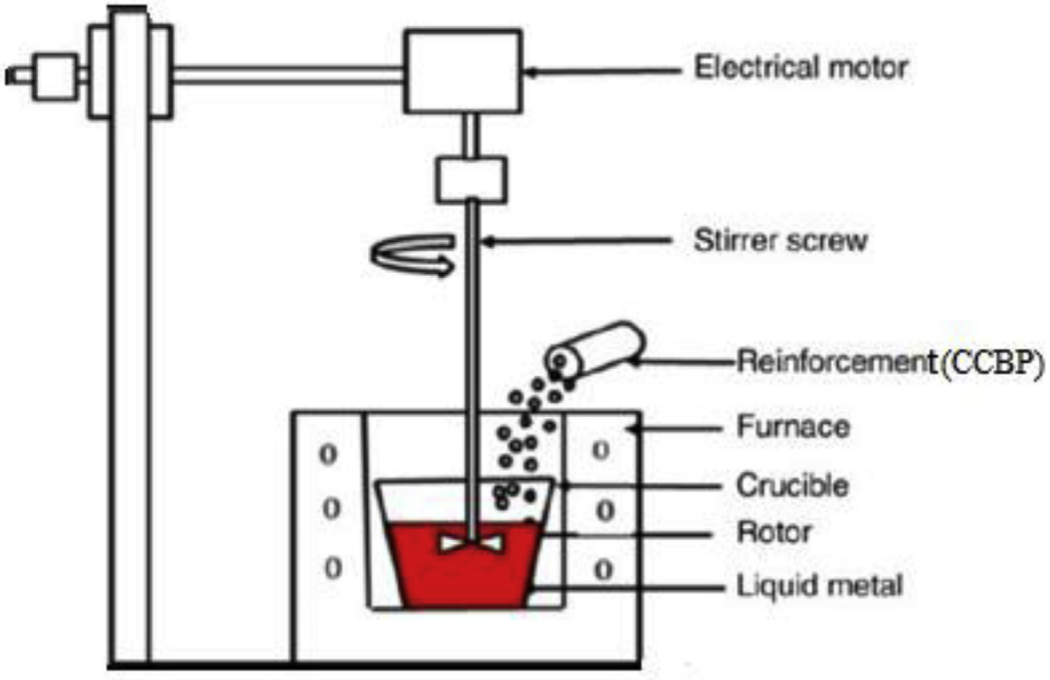

Fig. 1. Stir casting set up [30].

Fig. 2. Carbonized chicken bone powder.

2.3. A6063-CCBP composite preparation procedure

In this research, the stir casting was accomplished in a furnace with a peak temperature of 1000 °C (The maximum design temperature of the furnace used for the experiment). Production of Al6063-*CCBP* composite by stir casting technique involves liquefaction of matrix material, mixing of the ingredients and casting of the composite. A kilogram of A6063 ingots commercially available were deposited into the graphite crucible positioned in the stir cast setup. The ingot was dissolved to the liquid state by heat of the furnace to 650 °C. This was repeated for 95%, 90% and 85% A6063 ingots. A6063 matrix alloy was stirred constantly via the mechanical stirrer at 500 rpm for 15 min, and a vortex was produced in the crucible position in the furnace.

Nano sized CCBP was added in the amount of 0%, 5%, 10% and 15% weight as shown in Table 2 to the melted Al6063 alloy at the vortex, and melted composite slurry of varying proportions of Al6063-CCBP were prepared. The molten slurry was however transferred to a neat metallic die mould of dimension (100 × 100 x 10) mm at a pouring temperature ranging from 635 °C to 650 °C. The liquid composite was left for about 8.5 h to solidify at ambient temperature. Finally, the cast composite was taken from the die mould and prepared as samples for subsequent examinations.

2.4. Characterization of the cast aluminium alloy and cast composite samples

The Microstructural evaluations were carried with the aid of Scanning Electron Microscope (SEM) after etching the samples with 0.1 M HCl. Potentiodynamic polarization assessment and weight loss were used to characterize the corrosion behaviour of the samples. Mechanical properties of the samples such as hardness and tensile strenght were determined using Vickers hardness technique and tensile testing machine respectively. Electrical behaviours of the samples were obtained using the ammeter-voltmeter method.

Table 2
Weight percentage of Al6063 alloy and CCBP.

Samples	Al6063 (%)	CCBP (%)
A	100	0
B	95	5
C	90	10
D	85	15

2.4.1. Corrosion test

Autolab PGSTAT 101 Metrohm potentiostat equipped with NOVA software of version 2.1.2 was used for the potentiodynamic polarization experiment. This was carried out employing the three electrode system. The cast samples used for the experiment are of circular shape with diameter 20 mm and thickness 5 mm. The cast samples acting as the working electrode were mounted on resin and thereafter inserted into 0.5 M HCl solution at a room temperature of 25 °C. A graphite rod was used as the auxiliary electrode while silver chloride electrode was used as the reference electrode. The potential was scanned from −1.5 V OCP to 1.5 V OCP versus Ag/AgCl at a scan rate of 0.005 m/s and a step voltage of 0.00045 V. The experiment was repeated five times for each of the samples so as to ensure reproducibility in accordance to our previous work of ref. [31]. The weight loss experiment was also carried out by immersing each of the samples in 200 ml of prepared 0.5 M HCl solution at a room temperature for 3 days (72 h). The losses in mass of the specimen were recorded after every 12 h. In view of this, significant corrosion resisting ability of the cast aluminium composites were observed and compared to the cast aluminium alloy.

2.4.2. Microhardness test

The microhardness of the cast Al6063 and Al6063-CCBP composites of dimension (16 × 15 × 10) mm was investigated using Vickers hardness technique to obtain their indentation resistance. The samples were polished and subjected to a test load of 120 kgf for 15 s via pyramid-diamond indenter in accordance to ASTM: E384 Standard. The Vickers hardness testing machine is of Model HV114 with a square based diamond pyramid indenter that has a ground base of 136° between the opposite faces. Three different impressions were made with the applied load on the pyramid-shaped diamond indenter of the machine at various positions on the polished surface of each sample. The diagonal of the impressions are mapped and processed via the image processing methods that are inherent to the machine, and the VHNs of various samples were determined. The Vickers hardness numbers were computed from the apex angle of the pyramid indenter, diagonal of the impression measured, the load applied using the standard formula, presented in Eqn. (1) [33,34]. The indentation resisting effect of the reinforcing CCBP in the composites was compared at the conclusion of the test.

$$HV = \frac{2F\sin\left(\frac{136}{2}\right)}{n^2} = \frac{1.8544F}{n^2} \quad (1)$$

F is the impression load in kgf, n is the average diagonal of the impression in mm.

2.4.3. Tensile strenght test

The tensile strength test was carried out using UTM-6000 tensile test machine with servo control with the capacity of 600 kN. The tensile strength of the specimens was obtained by pulling them to failure in the computerized UTM-6000 tensile test machine. The test piece in the similitude of dog bone of length 100 mm. It has a cylindrical test region with the gauge length of 40 mm and diameter of 1.2 mm. Three different specimens of each sample were fabricated from the cast Aluminium alloy and composite of varying composition and pulled to rupture/breakage. The values of the average tensile strength were computed. The grip zone of test pieces was gripped to the jaws of the tensile testing machine and pulled by the applied force via the hydraulic drive. The test was carried out in accordance with ASTM: E0008 standards.

2.4.4. Electrical properties testing

The investigation of the electrical properties of the cast composites were carried out using the ammeter-voltmeter method. This is the simplest and fast method of measuring electrical resistance. It yields a moderately accurate value over a very wide range of resistances. The samples cut into dimension (20 × 10 x 5) mm were connected in a circuit with a voltmeter and ammeter as shown in Fig. 3. This enables the measurement of resistance and current when voltage was passed through the samples [35].

$$I = I_R + I_V \tag{2}$$

From Eqn. (2),

$$I_R = I - I_V \tag{3}$$

True value of unknown resistance is given by Eqn. (4)

$$R_x = \frac{V}{I_R} = \frac{V}{I - I_V} \tag{4}$$

Current through the unknown resistance can be written as Eqn. (5)

$$I_R = I\left(1 - V/IR_v\right) \tag{5}$$

V, voltmeter reading, R_v, resistance of voltmeter, and I, current indicated by the ammeter.

The measured value of resistance, $R_m = V/I$, which implies that $V/I = R_m$

Substituting $V/I = R_m$ into Eqn. (6), gives;

$$R_x = R_m\left(\frac{1}{1 - R_m/R_v}\right) \tag{7}$$

From Eqn. (7), it is clear that the true value of unknown resistance is equal to measured value of unknown resistance if voltmeter is of infinite resistance. However, if the voltmeter is of very large resistance as compared to the resistance under measurement.

$R_v >> R_m or R_m/R_v$ is very small.

$$\text{Therefore}, R_x = R_m[1 + (R_m/R_v)] \tag{8}$$

Thus, the measured value of unknown resistance, R_m is lesser than its true value.

$$\text{Relative error}, \varepsilon_r = (R_m - R_x)/R_x \tag{9}$$

3. Results and discussions

3.1. Potentiodynamic polarization measurements

The values of Ecorr (corrosion potential), jcorr (corrosion current density), R_P (polarization potential) and Cr (corrosion rate) of the cast samples in 0.5 M of HCl were gotten via the extrapolation of Tafel plot shown in Fig. 4. The results reveal the corrosion protection effect of the added CCBP in the test solution. The corrosion current density (jcorr) values of the Al6063-CCBP cast samples were found to be lesser than that of the Al6063 alloy cast. This indicates that the addition of CCBP blocked some of the active sites of the Al6063 alloy, minimizing exchange of current. The additive was able to provide inhibitive barriers, therefore limiting the cathodic evolution and anodic metal dissolution reactions of the metal matrix composite.

It is worthy of note that CCBP acted as a mixed inhibitor in Al6063- CCBP composite. This was affirmed by the close values of E_{corr}. Corrosion rate of sample D, with 85% Al6063 and 15% CCBP has the least corrosion rate of 0.4863 (mm/yr) as indicated in Table 3 while Sample A with 100% Al6063 and 0% CCBP has the highest corrosion rates. This could be traceable to the passivation tendency and chemical stability of the CCBP injected into the metal matrix alloy.

3.2. Weight loss results of the cast Al6063alloy and Al6063-CCBP composite

From the gravimetric studies, Sample A with 100% Al6063 and 0% CCBP was discovered to have experienced more weight loss than all other Samples during the 72 h of immersion in 0.5 M of HCl as presented in Fig. 5. Investigations and measurements made at 12 h interval reveal that the average weight loss by Sample D (85% Al6063 and 15% CCBP) was slightly lower than that of Sample C (90% Al6063 and 10% CCBP). The average weight loss by Sample B (95% Al6063 and 5% CCBP) was also found to be lower than that of Sample A but higher that weight loss by Sample C. This result is in conformity to the result obtained earlier from the potentiodynamic

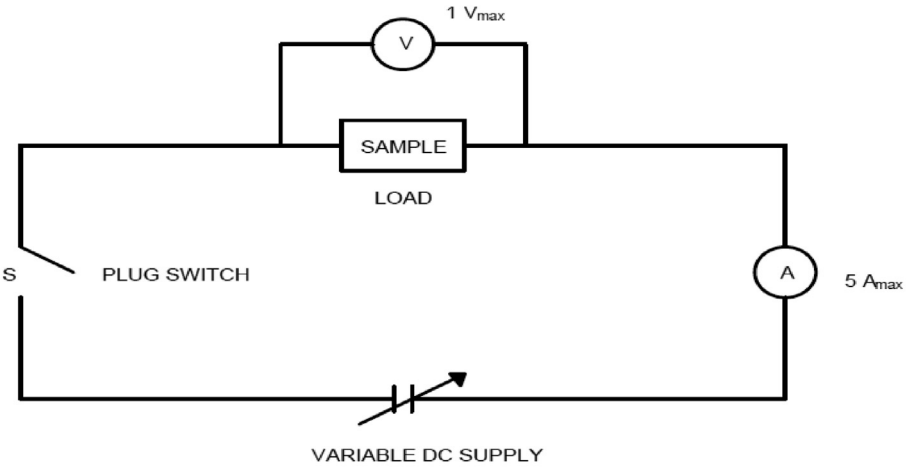

Fig. 3. Setup of the Electrical properties testing. Current through the ammeter = current through unknown resistance + current through voltmeter. This can be represented as Eqn. (2).

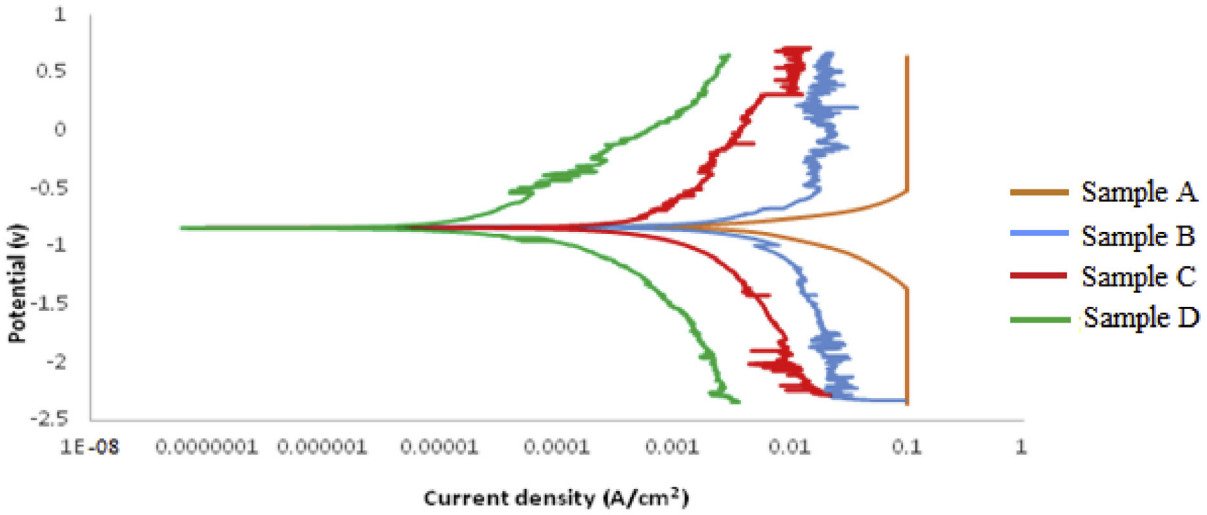

Fig. 4. Potentiodynamic polarization curves for Al6063 alloy and Al6063-CCBP composite.

Table 3
Potentiodynamic polarization data for Al6063 alloy and Al6063-CCBP composite.

Samples	jcorr (A/cm^2)	Rp(Ω)	E_{corr}(V)	Cr (mm/yr)
A	6.45E-05	36.39	−0.8328	0.7501
B	5.46E-05	150.24	−0.8308	0.6340
C	5.01E-05	170.26	−0.8289	0.5935
D	4.19E-05	205.21	−0.8247	0.4863

polarization experiment, which further attest to the corrosion protection ability of CCBP.

3.3. Microhardness behaviour Al6063 alloy and Al6063-CCBP composite

The Vickers microhardness results obtained for Al6063 alloy and Al6063-CCBP composite samples are presented in Fig. 6. Upon comparison Sample D with 85% Al6063 and 15% CCBP has the highest hardness value of 65.4 kgf/mm^2. Comparing the Vickers hardness numbers of the sample, addition of CCBP was seen to have had notable influence on the hardness of Al6063 alloy.

Fig. 6 indicates that the hardness value the base material increased from 52.86 kgf/mm^2 to 67.04 kgf/mm^2 which represents 26.83% increase in hardness. This improvement in the hardness of the alloy could be attributed to the high carbon content of the included CCBP. Furthermore, to examine the effect of CCBP addition in varying weight percentages, changes in the microhardness values from one level to the next were analysed and shown in Fig. 7. Notable increase in the microhardness value was noted for 10–15% CCPB composition compared to the 0–5 and 5–10% CCBP inclusion. This shows that the indentation resistance of the Al6063/CCBP composites increased due to the addition of CCBP. This study is in

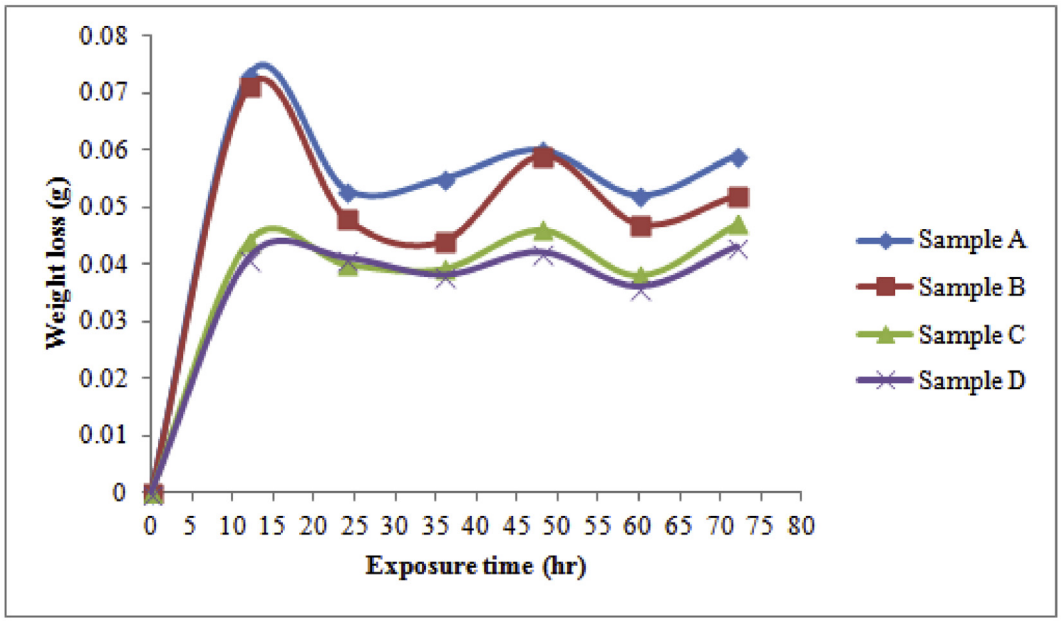

Fig. 5. Weight loss of Al6063 alloy and Al6063-CCBP composite.

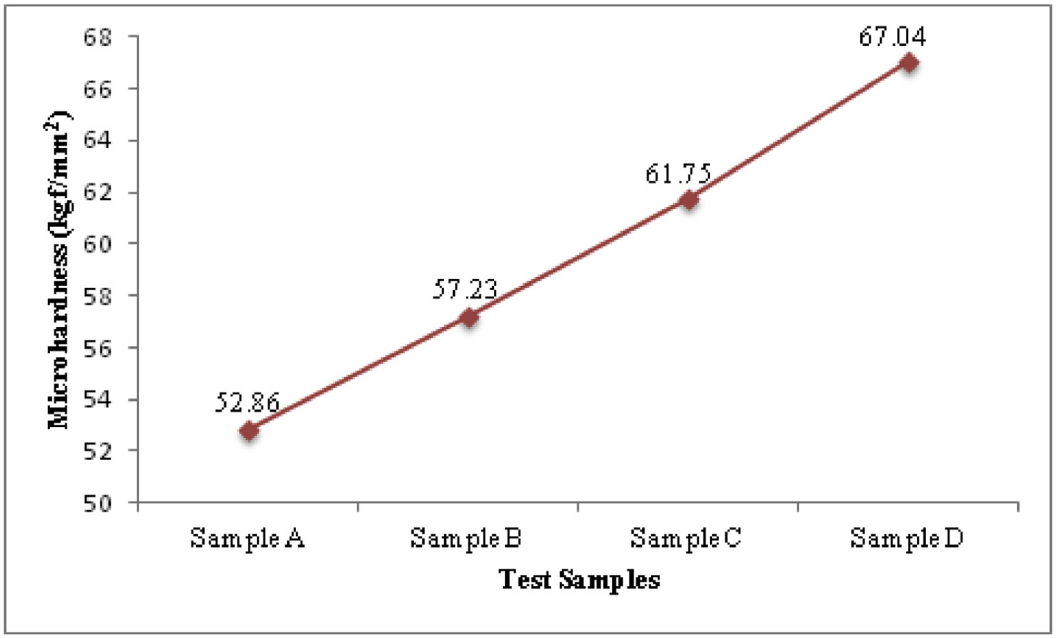

Fig. 6. Vickers microhardness of Al6063 alloy and Al6063-CCBP composite samples.

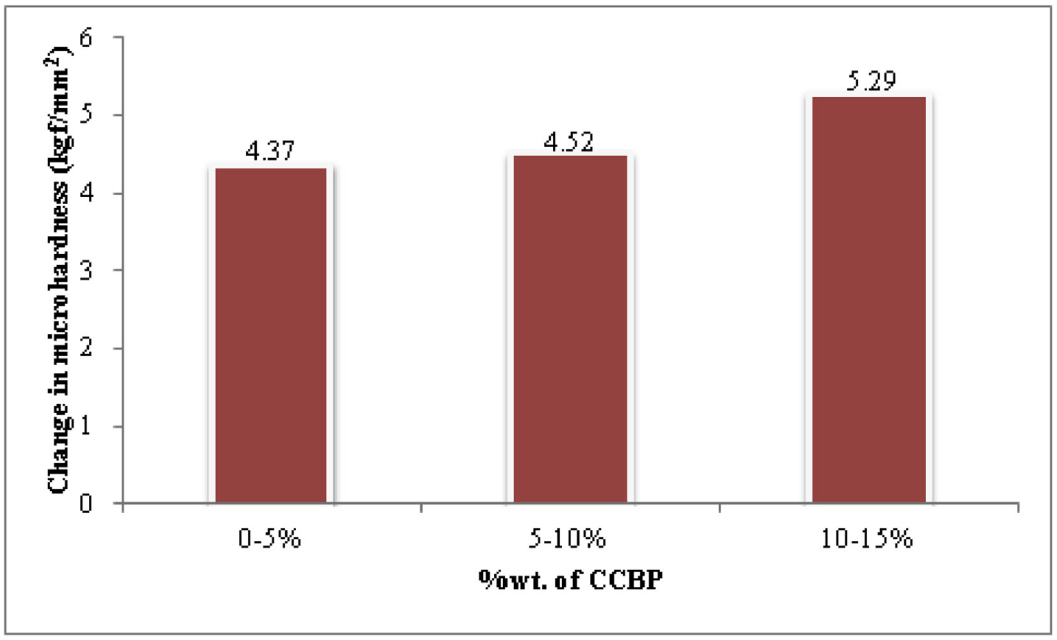

Fig. 7. Change in stage to stage comparison of microhardness.

par with the performance hardness characteristics recorded by [32].

3.4. Tensile strenght of Al6063 alloy and Al6063- CCBP composite

The average tensile strength results are shown in Fig. 8 for 0%, 5%, 10% and 15% addition. From the graph presented in Fig. 8 it can be seen that the values of the tensile strength increased from 138.42 N/mm^2 to 150.28 N/mm^2 when 5% of CCBP was added. Addition of 10% CCBP decreased the value of the tensile strength slightly. However, the tensile strength value further increased on the addition of 15% CCBP. These increments in tensile strength are a good indication that CCBP has the ability to reinforce A6063 alloy.

More so, the analysis of the effect of the addition of CCBP in percentage progression is presented in Fig. 9. A higher increase in the value of tensile strength was noticed between 10 and 15% inclusions of CCBP. The conflicting change in strength between 5 and 10% inclusion of CCBP could be attributed to the phenomenon that result in a reduction in the ductility of composite in micro level locality near the CCBP [36].

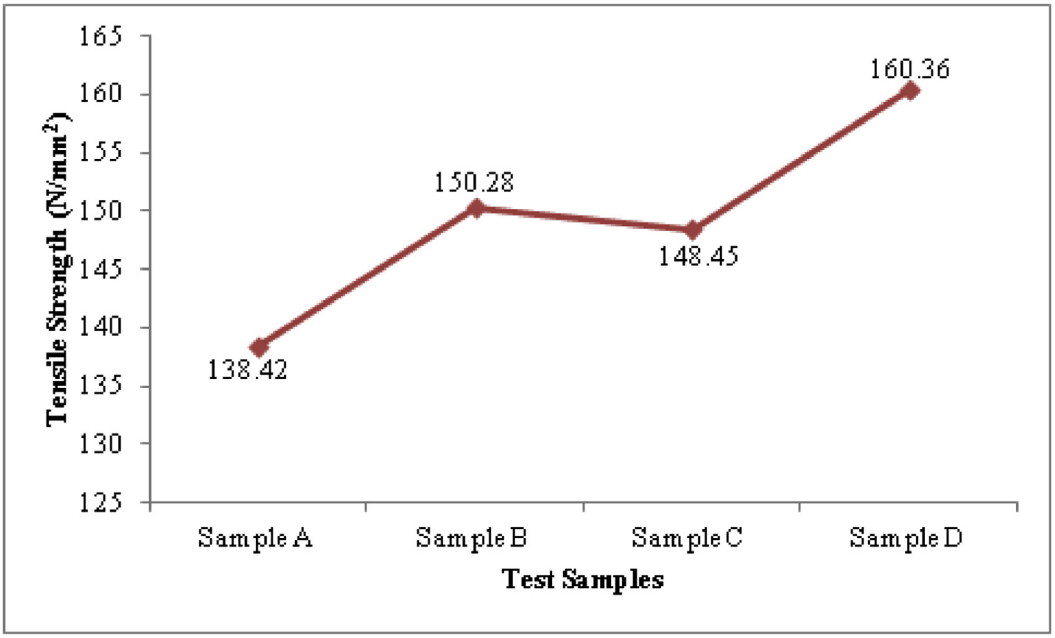

Fig. 8. Tensile Strenght of Al6063 alloy and Al6063-CCBP composite samples.

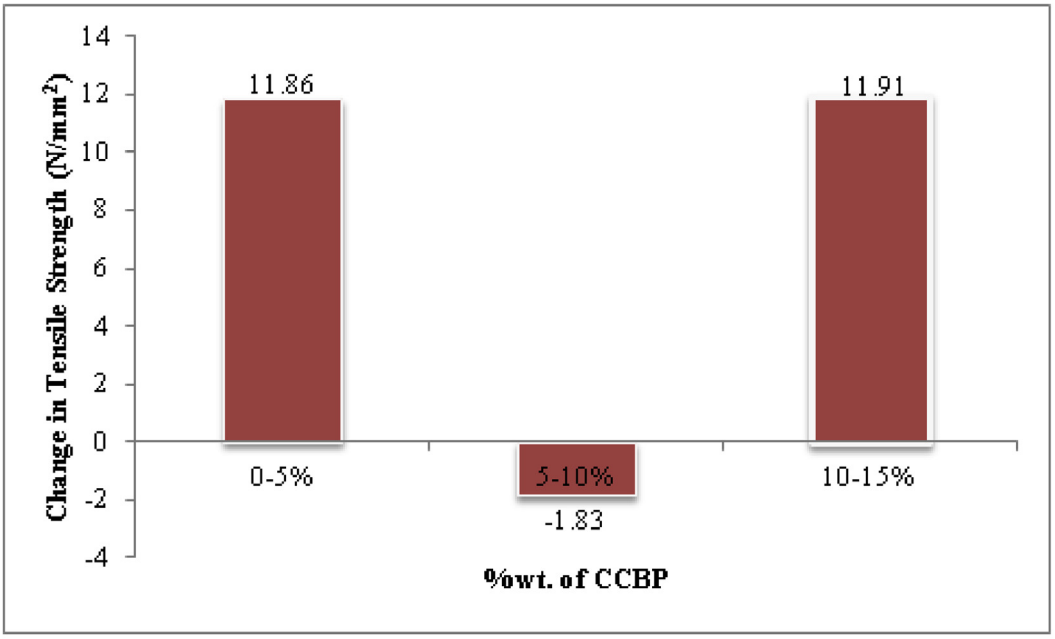

Fig. 9. Change in stage to stage comparison of Tensile Strenght.

3.5. *Effect of CCBP on the electrical property of A6063 alloy*

The electrical test conducted on the composite reveal that CCBP insulated the Aluminium matrix. The maximum current of 2.0 A were made to flow through the samples. It was observed as shown in Fig. 10 that the aluminium alloy posses the lowest electrical resistivity of 0.4 Ωmm while sample D with 85% Al6063 and 15% CCBP has the highest electrical resistivity value of 2.2 Ωmm. The values of electrical resistivity were found to increase on the addition of the various percentage weight of CCBP. This result affirms the doping ability of CCBP against the flow of electricity.

Furthermore, the analysis of the electrical conductivity on the inclusion of CCBP to the metal matrix is shown graphically in Fig. 11. Expectedly, electrical conductivity of the samples is in reverse order compared to the resistivity. Sample A with 100% Al6063 and 0% CCBP has the greatest electrical conductivity of 2.5 $(\Omega mm)^{-1}$ and the least was found with Sample D that comprises 85% Al6063 and 15% CCBP with electrical conductivity of 0.45 $(\Omega mm)^{-1}$. This further confirms the insulating effect of CCBP on the metal matrix composite.

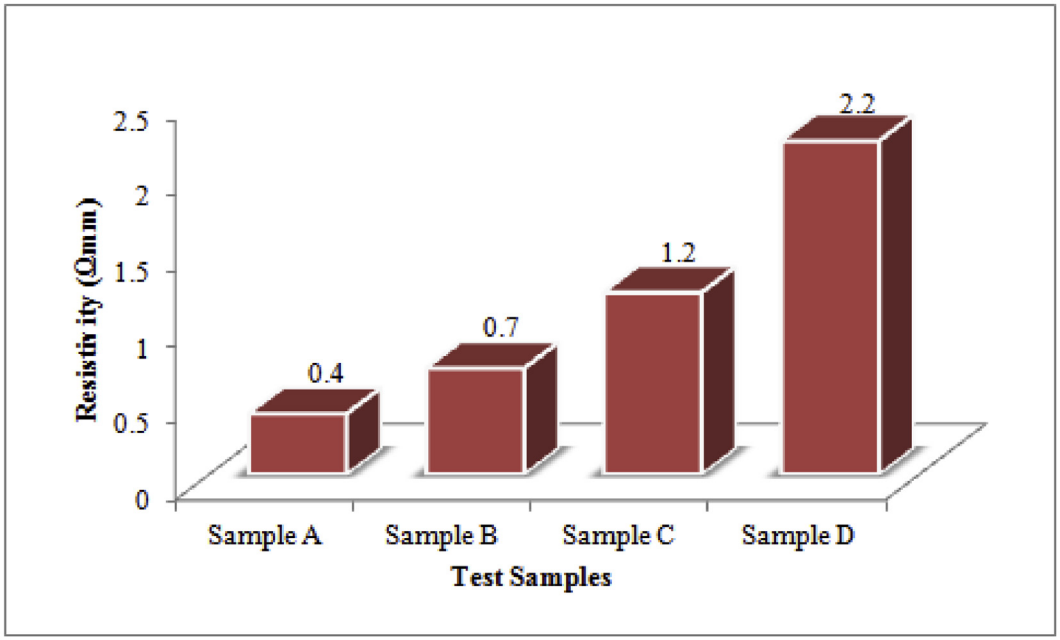

Fig. 10. Electrical resistivity of Al6063 samples with various %wt. of CCBP.

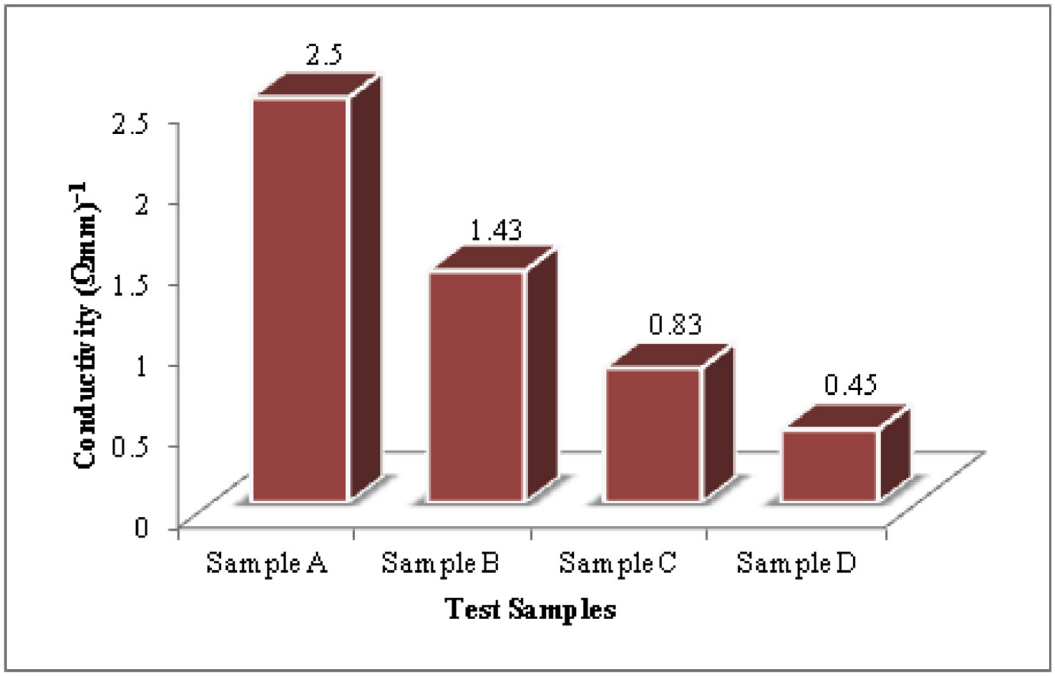

Fig. 11. Electrical conductivity of Al6063 samples with various %wt. of CCBP.

3.6. Morphology and structure analysis of Al6063 and Al6063-CCBP samples

The SEM micrograph of 0%, 5%, 10% and 15% inclusion of CCBP are shown in Fig. 12a–d. The presence of the reinforcing CCBP in the Al6063/CCBP composite was observed in Fig. 12b–d. The Micrographs indicated that the CCBP were homogenously dispersed with low agglomeration at the matrix and the distributions are in proportion of the percentage addition in the cast composite.

The SEM images indicate that the inclusion of CCBP minimise the grain size of aluminum matrix. The grain size of the matrix of a nanocomposite material is dependent on the particles volume fraction and size. It can be noticed in Fig. 12b–d that the addition of CCBP with nano particle size decrease the grain size of the Aluminium matrix. The decrease grain size could be attributed to the greater percentage of grain boundary which limits grain growth [37]. Minimal micro porosities were observed in the between the grain boundary region of the SEM micrograph shown in Fig. 12b–d compared to Fig. 12a. The decrease in porosities and cleavages could be traceable to the inclusion of CCBP, thereby leading to reduction

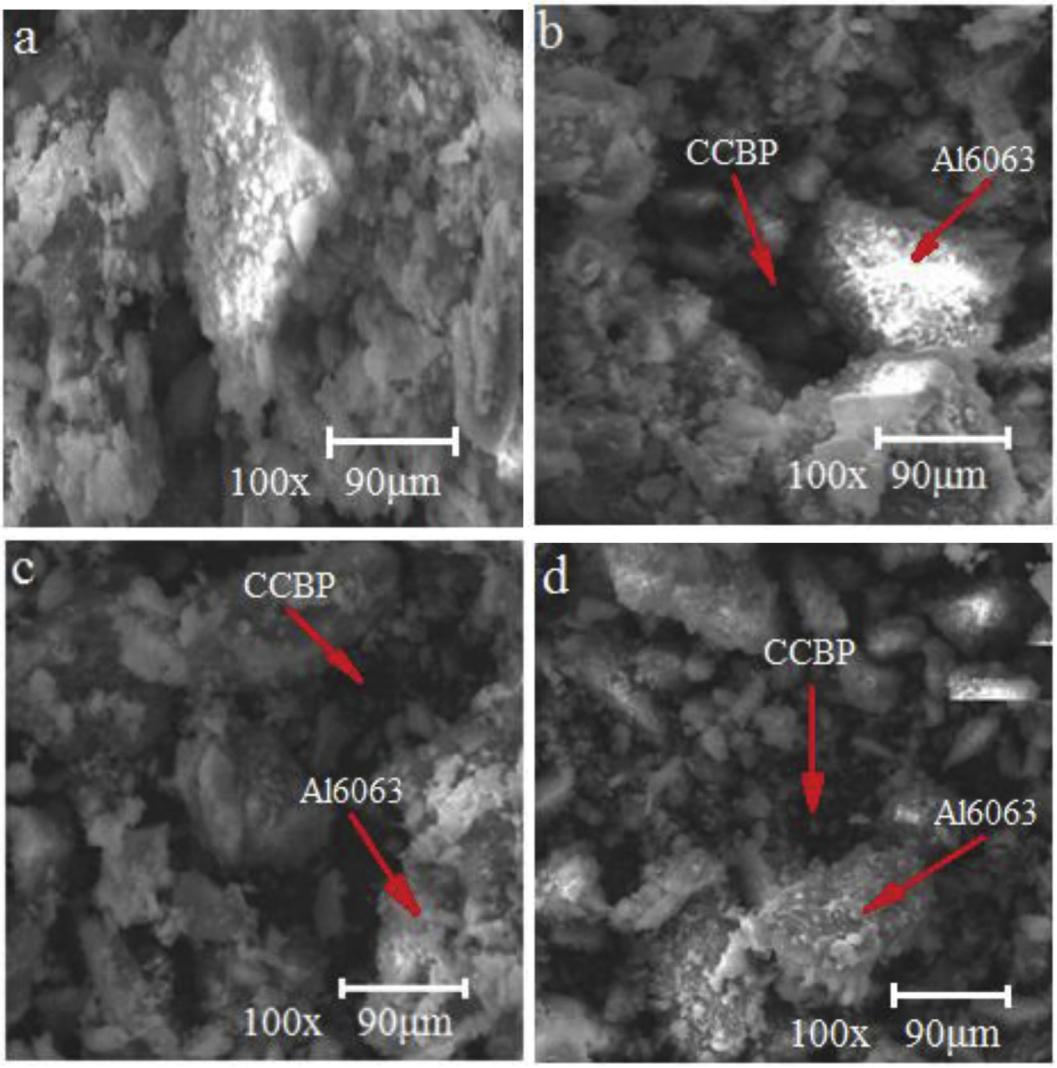

Fig. 12. SEM micrograph of (a) Sample A (Al6063) (b) Sample B (95%Al6063 + 5% CCBP) (c) Sample C (90%Al6063 + 10% CCBP) (d) Sample D (85% Al6063 + 15% CCBP).

in the entrapment of gases during casting [38,39]. As indicated in Fig. 12a there is an active re-crystallization in Al6063 by the generation of brand-new grains in the prior grain boundaries. However, in Fig. 12b–d the recrystallization level subsided as the percentage weight of CCBP increases, acting as barrier to the migration of grain boundary.

4. Conclusions

The outcomes of the addition of CCBP in A6063-CCBP composites were examined when subjected to corrosive medium, hardness and tensile test. The following conclusion was drawn from the experimental result:

- The reinforcement of Al6063 aluminium metal matrix with CCBP of varying percentage weight via stir casting shows a significant impact on the performance characteristics of the composites.
- The electrochemical and gravimetric experiment shows that the corrosion resistance of the composite increase as the percentage of CCBP increases.
- The values of the Vickers's hardness of the composites rise with the increase in percentage concentration of CCBP with about 26.83% increase on the addition of 15% CCBP. In the same vein, the tensile strength increases on the addition of different percentages of CCBP.
- Ultimately, the morphological change via SEM (Scanning Electron Microscope) micrograph unveiled that the inclusion of CCBP in the Al6063 metal matrix reduced cleavages, showing uniform dispersion of the reinforcement along the grain boundaries and more so, minimised brittle fracture.

Acknowledgement

The authors acknowledged the Surface Engineering Research Centre, Department of Mechanical Engineering, Covenant University Ota for providing the necessary research facility.

References

[1] I. Balasubramanian, R. Maheswaran, Effect of inclusion of SiC particulates on the mechanical resistance behaviour of stir-cast AA6063/SiC composites, Mater. Des. (1980–2015) 65 (2015) 511–520.
[2] A.A. Ayoola, V.E. Efeovbokhan, O.T. Bafuwa, O.T. David, A search for alternative solvent to hexane during neem oil extraction, Int. J. Sci. Technol. 4 (4) (2014) 66–70.
[3] I.G. Akande, O.O. Oluwole, O.S.I. Fayomi, Optimizing the defensive characteristics of mild steel via the electrodeposition of Zn-Si_3N_4 reinforcing particles,

Def. Technol. (2018). https://doi.org/10.1016/j.dt.2018.11.00.
[4] S. Alkahtani, Mechanical performance of heat treated 319 alloys as a function of alloying and aging parameters, Mater. Des. 41 (2012) 358–369.
[5] M.F. Ibrahim, E. Samuel, A.M. Samuel, A.M. Al-Ahmari, F.H. Samuel, Metallurgical parameters controlling the microstructure and hardness of Al–Si–Cu–Mg base alloys, Mater. Des. 32 (4) (2011) 2130–2142.
[6] M. Dave, K. Kothari, Composite material-aluminium silicon alloy: a review, Paripex - Indian J. Res. 2 (3) (2013) 148–150.
[7] O.S.I. Fayomi, I.G. Akande, A.P.I. Popoola, Corrosion protection effect of chitosan on the performance characteristics of A6063 alloy, J. Bio-Tribo-Corrosion 4 (4) (2018) 73.
[8] B.A. Kumar, N. Murugan, Metallurgical and mechanical characterization of stir cast AA6061-T6–AlNp composite, Mater. Des. 40 (2012) 52–58.
[9] A.P. Subrahmanyam, J. Madhukiran, G. Naresh, S. Madhusudhan, Fabrication and characterization of Al356. 2, rice husk ash and fly ash reinforced hybrid metal matrix composite, Int. J. Adv. Sci. Technol. 94 (2016) 49–56.
[10] F.A. Raju, M.D. Kumar, Experimental investigation on MRR in abrasive water jet machining of AL 7075-T6 and fly ash metal matrix composite 6 (5) (2017) 2277–5668.
[11] M.O. Durowoju, J.O. Agunsoye, L.O. Mudashiru, A.A. Yekinni, S.K. Bello, T.O. Rabiu, Optimization of stir casting process parameters to improve the hardness property of Al/RHA matrix composites, Eur. J. Eng. Res. Sci. 2 (11) (2017) 5–12.
[12] R. Dasgupta, Aluminium alloy-based metal matrix composites: a potential material for wear resistant applications, ISRN Metall. 2012 (2012) 14, https://doi.org/10.5402/2012/594573. Article ID 594573.
[13] J.P. Park, M.G. Kim, U.S. Yoon, W.J. Kim, Microstructures and mechanical properties of Mg–Al–Zn–Ca alloys fabricated by high frequency electromagnetic casting method, J. Mater. Sci. 44 (1) (2009) 47–54.
[14] A. Kitahara, S. Akiyama, H. Ueno, M. Sakamoto, H. Hirai, Development of noncombustible magnesium alloys, Mater. Jpn. (Jpn.) 39 (1) (2000) 72–74.
[15] S. Guo, Q. Le, Z. Zhao, Z. Wang, J. Cui, Microstructural refinement of DC cast AZ80 Mg billets by low frequency electromagnetic vibration, Mater. Sci. Eng., A 404 (1–2) (2005) 323–329.
[16] P. Li, B. Tang, E.G. Kandalova, Microstructure and properties of AZ91D alloy with Ca additions, Mater. Lett. 59 (6) (2005) 671–675.
[17] N. Rugayah, H. Nuraini, Chicken bone charcoal for defluoridation of groundwater in Indonesia, Int. J. Poultry Sci. 13 (10) (2014) 591–596.
[18] B. Suárez-Peña, J. Asensio-Lozano, J.I. Verdeja-Gonzalez, J.A. Pero-Sanz Elorz, Microstructural effects of phosphorus on pressure die cast Al-12Si components, Rev. Metal. 43 (5) (2007 Jan 1) 352–358.
[19] E. Doernberg, A. Kozlov, R. Schmid-Fetzer, Experimental investigation and thermodynamic calculation of Mg-Al-Sn phase equilibria and solidification microstructures, J. Phase Equilibria Diffusion 28 (6) (2007) 523–535.
[20] B.A. Kumar, N. Murugan, Metallurgical and mechanical characterization of stir cast AA6061-T6–AlNp composite, Mater. Des. 40 (2012) 52–58.
[21] M.O. Shabani, A. Mazahery, The synthesis of the particulates Al matrix composites by the compocasting method, Ceram. Int. 39 (2) (2013) 1351–1358.
[22] A. Kumar, M.M. Mahapatra, P.K. Jha, Fabrication and characterizations of mechanical properties of Al-4.5% Cu/10TiC composite by in-situ method, J. Miner. Mater. Char. Eng. 11 (11) (2012) 1075.
[23] S.B. Boppana, K. Chennakeshavalu, Preparation of Al-5Ti master alloys for the in-situ processing of Al-TiC metal matrix composites, J. Miner. Mater. Char. Eng. 8 (07) (2009) 563.
[24] A. Albiter, C.A. Leon, R.A. Drew, E. Bedolla, Microstructure and heat-treatment response of Al-2024/TiC composites, Mater. Sci. Eng. 289 (1–2) (2000) 109–115.
[25] M. Singla, D.D. Dwivedi, L. Singh, V. Chawla, Development of aluminium based silicon carbide particulate metal matrix composite, J. Miner. Mater. Char. Eng. 8 (06) (2009) 455.
[26] S.B. Hassan, V.S. Aigbodion, The study of the microstructure and interfacial reaction of Al–Cu–Mg/bagasse ash particulate composite, J. Alloys Compd. 491 (1–2) (2010) 571–574.
[27] J.E. Oghenevweta, V.S. Aigbodion, G.B. Nyior, F. Asuke, Mechanical properties and microstructural analysis of Al–Si–Mg/carbonized maize stalk waste particulate composites, J. King Saud Univ. Eng. Sci. 28 (2) (2016) 222–229.
[28] M. Kok, Production and mechanical properties of Al2O3 particle-reinforced 2024 aluminium alloy composites, J. Mater. Process. Technol. 161 (3) (2005) 381–387.
[29] M. Ramachandra, K. Radhakrishna, Sliding wear, slurry erosive wear, and corrosive wear of aluminium/SiC composite, Mater. Sci. Wroclaw 24 (2/1) (2006) 333.
[30] A.A. Ahamed, R. Ahmed, M.B. Hossain, M. Billah, Fabrication and characterization of aluminium rice husk ash composite prepared by stir casting method, Rajshahi univ. J. Sci. Technol. 44 (2016) 9–18.
[31] O.S.I. Fayomi, I.G. Akande, O.O. Oluwole, D. Daramola, Effect of water-soluble chitosan on the electrochemical corrosion behaviour of mild steel, Chem. Data Collect. 1 (17) (2018) 321–326.
[32] Krishna, M. Karthik, Evaluation of hardness strength of aluminium alloy (AA6061) reinforced with silicon carbide, Int. J. Recent Technol. Mech. Electr. Eng. 1 (4) (2014) 14–18.
[33] O. Uzun, T. Karaaslan, M. Gogebakan, M. Keskin, Hardness and microstructural characteristics of rapidly solidified Al–8–16 wt.% Si alloys, J. Alloys Compd. 376 (1–2) (2004) 149–157.
[34] I.L. Denry, J.A. Holloway, Elastic constants, Vickers hardness, and fracture toughness of fluorrichterite-based glass–ceramics, Dent. Mater. 20 (3) (2004) 213–219.
[35] K.F. Ayarkwa, S.W. Williams, J. Ding, Assessing the effect of TIG alternating current time cycle on aluminium wire arc additive manufacture, Addit. Manuf. 18 (2017) 186–193.
[36] I. Balasubramanian, R. Maheswaran, Effect of inclusion of SiC particulates on the mechanical resistance behaviour of stir-cast AA6063/SiC composites, Mater. Des. (1980–2015) 65 (2015) 511–520.
[37] H.R. Ezatpour, S.A. Sajjadi, M.H. Sabzevar, Y. Huang, Investigation of microstructure and mechanical properties of Al6061-nanocomposite fabricated by stir casting, Mater. Des. 55 (2014) 921–928.
[38] M.K. Akbari, O. Mirzaee, H.R. Baharvandi, Fabrication and study on mechanical properties and fracture behavior of nanometric Al_2O_3 particle-reinforced A356 composites focusing on the parameters of vortex method, Mater. Des. 46 (2013) 199–205.
[39] A. Alizadeh, E. Taheri-Nassaj, M. Hajizamani, Hot extrusion process effect on mechanical behavior of stir cast Al based composites reinforced with mechanically milled B4C nanoparticles, J. Mater. Sci. Technol. 27 (12) (2011) 1113–1119.